Available online at www.sciencedirect.com
ScienceDirect
Catalysis Today 127 (2007) 219–229
CATALYSIS TODAY
www.elsevier.com/locate/cattod

Behaviour of SO_x-traps derived from ternary Cu/Mg/Al hydrotalcite materials

Gabriele Centi *, Siglinda Perathoner

Department of Industrial Chemistry and Engineering of Materials of the University of Messina and ELCASS (European Laboratory for Catalysis and Surface Science), Salita Sperone 31, 98166 Messina, Italy

Available online 18 May 2007

Abstract

Cu/Mg/Al ternary HT-derived materials show significantly better SO_x trap performances with respect to binary Cu/Al HT-derived materials and represent an interesting type of material either to protect NO_x traps from the deactivation by sulphur or as SO_x additives in fluid catalytic cracking (FCC) applications. The kinetics of SO_2 uptake was studied at low (10 ppm) and higher (1000 ppm) SO_2 concentration in a thermobalance (TG) apparatus. The results were compared with those obtained by measuring the SO_2 breakthrough curves in a flow reactor under reaction conditions simulating those of autoexhaust gases, in particular regarding the use of high space-velocities and the presence of CO_2 in the feed. The SO_x trap performances depend on the feed composition and type of experiments. However, a similar ranking of the SO_x trap performances was observed for the different configurations. Cu/Mg/Al = 1:1:2 shows the best performance and also improved hydrothermal stability with respect to Cu/Al binary samples.

Keywords: SO_2; SO_x trap; Copper; Hydrotalcite; Cu/Mg/Al mixed oxides; FCC; NO_x trap protection

1. Introduction

There is a significant recent interest in developing advanced SO_x traps for protecting NO_x traps from deactivation by sulphur or as additives to reduce SO_x emissions in fluid catalytic cracking (FCC) units. Various recent patents claim the use of SO_x traps based on transition metal mixed oxides to protect the NO_x-storage catalyst (NO_x trap) from the deactivation by sulphur compounds present in the exhaust gases of diesel or lean-burn gasoline engines [1–11]. In fact, the performances of NO_x-storage reduction catalysts, the life-time, the engine management and fuel economy could be significantly improved by removing SO_x from the engine exhaust gases prior to the contact with the NO_x trap. This solution was not feasible few years ago, but the low sulphur content fuel available already on the market (around 10 ppm) makes technically feasible the use of a disposable or ex situ regenerable SO_x trap [12].

Even if the SO_x trap is not completely efficient in the removal of sulphur compounds before the contact of the emissions with the NO_x traps, there are still benefits in using the SO_x/NO_x traps combination, because the periodic regeneration of NO_x trap can be made in less severe reaction conditions (in terms of time and temperature, and λ value, e.g. air to fuel ratio). There is a consequent decrease of: (i) fuel consumption, (ii) formation of toxic side-products such as H_2S and COS, and (iii) rate of deactivation of the NO_x trap due to both a reduction in the progressive fraction of noble metal irreversibly deactivated (essentially due to the formation of PtS like species) and to a lower sintering rate.

Relatively few fundamental studies have been published on the development of these SO_x traps, but the interest is growing recently. Fricke and co-workers [13,14] reported the behaviour of different SO_x trap materials based on mesoporous Al_2O_3 supports modified with storage components (Ca or Ba) and oxidation components (Pt, Cu or Mn). In particular, Ca-Al mixed oxide-based materials doped with Na and Mn were found as very efficient S trapping materials [14]. Wokaun and co-workers [15] have analyzed the storage of SO_2 in Mn-based materials observing that the storage of SO_2 in pure and K-doped Mn oxide is controlled by the kinetics of the sulphate formation reaction on the catalyst surface up to complete sulphation, whereas the storage on Mn-Ce mixed oxide is limited by

* Corresponding author. Tel.: +39 090 676 5609; fax: +39 090 391518.
E-mail address: centi@unime.it (G. Centi).

0920-5861/$ – see front matter © 2007 Elsevier B.V. All rights reserved.
doi:10.1016/j.cattod.2007.04.009

internal diffusion of the formed sulphate. Lercher and co-workers [16] have analyzed the behaviour in SO_2 adsorption of Ba-doped metal organic framework (MOF) materials with Cu^{2+} as central cation and benzene-1,3,5-tricarboxylate (BTC) as linker. The same group [17] has also investigated as SO_x traps different mesoporous or layered materials (MCM-22, MCM-36 and ITQ-2) modified with a storage element (Ba, Al, or Mg) and an oxidation component (Pt). The mechanism of SO_x trapping was also studied in detail by this group [18–21].

Li and King [22] have studied SO_2 adsorbents based on manganese oxide octahedral molecular sieves. Limousy et al. [23] have analyzed the performances of commercial cordierite-type monoliths (the washcoat contains noble metals, Ba, Cr, Zr as the key components). Wang et al. [24] have investigated a Mg-Fe-Al-O mixed oxide with spinel structure, while Iretskaya and Mitchell [25], Hao and Cooper [26] and Centi et al. [27] analyzed copper-on-alumina materials for the sorption of SO_2.

Therefore, different materials have been studied in literature, but the use of different testing procedures does not allow a clear identification of the preferable type of material to prepare SO_x traps. A main difficulty in the comparison arises also from the absence of a clear relationship of the SO_x trap features with the kinetic regime determining the performances. In studying and modelling the kinetics of SO_2 adsorption and SO_x bulk diffusion on a reference ''state-of-the-art'' SO_x trap [28] (a 2% Pt on alumina doped with various alkaline and alkaline-earth metals) we have shown that at low temperature (200 °C) the behaviour depends on the slow solid-state diffusion of the sulphate species. Above 300 °C the rate depends initially on the surface reaction, but after the saturation of the surface the solid-state diffusion dominates again the performances in SO_2 uptake. The sulphation process $MO + 0.5O_2 + SO_2 \rightarrow MSO_4$ determines an increase in the cell volume of about 30–40%. Therefore, after the sulphation of the first surface layers the progress of the reaction is difficult, because it requires a solid-state rearrangement. Even diffusion in the micropores becomes inhibited. Therefore, a structure more ''flexible'' to accommodate this change could improve the SO_x trap performances.

Following this concept, we have shown in a previous contribution [29] that using Cu-Al mixed oxides derived from hydrotalcite (HT) precursors it is possible to obtain superior performances with respect to the cited reference SO_x traps, thanks also to their characteristics of ''memory effect'', e.g. their capacity of reforming the hydrotalcite structure at medium temperature in the presence of CO_2. In fact, an analogy between the sulphate and carbonate groups is observed in hydrotalcite materials [30,31] and the possibility of ''easy'' reconstruction of the HT structure of mildly calcined samples upon exposure to CO_2 implies an easy rearrangement during the process of sulphation, e.g. an easier process of bulk sulphation. The possibility of continuous reconstruction and decomposition of the HT-derived structure deriving from the fluctuations in the temperature of the exhaust gases from the engine is also a mechanism, which could be relevant regarding their stability during operation. Furthermore, HT-derived materials offer a great flexibility of tuning by substitution of bi- and tri-valent elements. To note, however, that the HT is not the effective structure of the SO_x trap, but only the precursor. Typical temperature operations for SO_x traps are up 500–600 °C and therefore they should be calcined at least to 500 °C prior their testing. In these conditions, the HT-structure transforms to a typically amorphous mixed oxide [31].

The aim of this contribution is to analyze whether the use of ternary (Cu-Mg-Al) mixed oxides derived from hydrotalcite precursors could improve the performances with respect to those of binary Cu-Al-oxides SO_x traps previously reported [29]. To note that noble metals are absent in these SO_x traps, and in general their preparation is low cost, making thus possible their use also as disposable SO_x traps. To mention, is also that a further motivation to investigate this type of material derives from the possibility to develop double-layered NO_x traps catalysts [32], in which the external layer has the function of SO_x trap and a composition close to that investigated here (for example, $MgAl_2O_4$ or $MgAl_2O_4{\cdot}CeO_2$ in Ref. [32b]). HT-derived NO_x traps have been shown to have interesting performances comparable to those of the commercial samples [33,34].

HT-derived materials have been show to be also high-efficient SO_x additives in fluid catalytic cracking applications [35–38], in the simultaneous catalytic removal of NO_x, SO_x, and CO under FCC regenerator conditions [39] and in the removal of SO_x from flue gas from refinery or energy production [40–42]. Two short reviews, although in Chinese, have been published recently on the application of HT-derived compounds in the catalytic removal of SO_2 and NO_x in flue gas [43,44]. There is in general high interest on new FCC SO_x additives [45–49], especially when they could combine also the reduction of NO during regeneration of spent FCC catalyst [50–52]. The results of the investigation reported here could be thus relevant also to the development of novel FCC additives.

2. Experimental

2.1. Preparation of the SO_x traps

The SO_x traps were prepared by calcination of hydrotalcite-like (HT) compounds with general formula $[Cu_{1-x-y}Mg_yAl_x(OH)_2]^{x+}(A_{x/n}{}^{n-})\cdot mH_2O$. The HT compound has been obtained by coprecipitation at 60 °C and controlled pH of 9.5–10, using Na_2CO_3 as the precipitation agent. The M(II) and M(III) cations were added to the aqueous solution as the corresponding nitrate salts. During precipitation, the pH was kept constant by adding NaOH 3 M or HNO_3 conc. The obtained hydrotalcites, after aging at 60 °C overnight, have been washed with hot distilled water until complete Na^+ elimination. The precipitates were then dried at 90 °C for 4 h and subsequently calcined at 500 °C for 5 h.

Two Cu/Mg/Al HT-derived compounds were prepared, the first with a Cu/Mg/Al ratio of 1:1:2 and the second with a Cu/Mg/Al ratio of 1:2:1. For reference, also two binary Cu/Al HT-derived compounds were also prepared, with a Cu/Al ratio of 1:2 and 1:3, because these were found the preferable Cu/Al ratios when we studied the performances of these binary HT-derived compounds [29]. Table 1 summarizes the compositions and BET surface area of the samples investigated.

Table 1
Cu/Mg/Al ratio and surface area of the SO_x trap used in this work

Sample formal composition	Cu/Mg/Al ratio	Surface area before calcination[a] (m^2/g)	Surface area after calcination 500 °C (m^2/g)
$Cu_{0.80}Mg_{0.80}Al_{1.6}O_4$	1:1:2	90	80
$Cu_{0.89}Mg_{1.78}Al_{0.89}O_4$	1:2:1	124	111
$Cu_{0.47}Al_{2.35}O_4$	1:0:3	234	216
$CuAl_2O_4$	1:0:2	258	242

[a] Surface area after drying, before calcination.

2.2. Characterization

The BET surface area was measured using nitrogen sorption at 77 K. Prior to the experiments, the samples were outgassed at 100 °C for 5 h. The isotherms were measured using a Micrometrics ASAP 2010 system.

X-ray diffraction (XRD) patterns were recorded with an Ital-Structures XRD diffractometer using Cu Kα radiation (λ = 1.5405 Å).

Scanning electron microscope (SEM) images were recorded with a JEOL 5600 LV equipment. Elemental analysis was carried out via energy dispersion analysis using an X-ray analytical system EDX OXFORD, coupled to the scanning electron microscope.

2.3. Reactivity tests

The kinetic of adsorption of the SO_x traps was analyzed in a thermobalance (TG) flow apparatus (TGA Q50 from TA Instruments) characterized by a tangential flow of the reactive gas just above the pan containing about 10 mg of the sample in the form of fine powder. This configuration allows a quite fast response to changes in the inlet flow composition. The experiments were typically made under isothermal conditions, after pre-treatment of the sample at 500 °C to eliminate adsorbed substances. The catalyst was then cooled down up to the requested temperature in a flow of N_2, and after reaching a constant weight, the flow was switched from N_2 to air containing 0.1% SO_2, monitoring the change of weight as a function of time on stream.

Breakthrough curves of SO_2 uptake in reaction conditions close to those of diesel engine emissions were made in a flow reactor apparatus formed by (i) a section of feed control using mass flowmeters and already calibrated gas mixtures stored in cylinders, (ii) a quartz tubular reactor of internal diameter of about 10 mm in which the SO_x trap, in the form of small grains of about 0.1 mm diameter (typically 40 mg), is put in the middle between two glass–wool layers; the quartz tube is then inserted in an electrically heated tubular oven, and (iii) a section for on-line continuous analysis achieved by a FTIR spectrometer equipped with a gas cell of 10 m of (multiple) path length (total volume of the cell is 0.7 l). The SO_2 bands at 1346 and 1369 cm^{-1} were monitored; quantitative data were obtained using a periodic calibration with standard mixtures of known composition. The tests were made at a volumetric flow rate of 30 l/h which corresponds to a space-velocity of 150,000 h^{-1} (around 500,000 h^{-1} considering a catalyst bed void fraction of 0.3). The feed composition was the following: 20 ppm SO_2, 11% CO_2, 5% O_2, remaining N_2.

To analyze the stability of the materials, the samples were first subjected to a hydrothermal treatment (6 h at 600 °C in the presence of a flow containing 11% CO_2, 5% O_2, 5–7% H_2O and the remaining N_2) before determining the breakthrough curves of SO_2 uptake.

3. Results and discussion

3.1. Characterization

The surface area of the samples is reported in Table 1. The surface area of the ternary materials upon calcination is around 100 m^2/g, although about 30% lower for Cu/Mg/Al = 1:1:2 with respect to 1:2:1 sample. The calcination does not cause a significant decrease of the surface area with respect to the sample after drying. The surface area of the ternary materials is about 2–3 times lower with respect to that of the Cu/Al binary HT-derived materials.

X-ray diffraction pattern of the ternary materials (Cu/Mg/Al oxides with ratio 1:1:2 and 1:2:1) before calcination indicates the presence of nearly amorphous materials (Fig. 1). Only weak and very broad lines could be detected near $2\theta = 37°$, 43° and 63° possibly indicating the presence of small crystalline MgO particles, even if the peaks are too broad for any conclusion. After calcination at 500 °C and cooling in an inert atmosphere, the samples remain amorphous, but leaving them exposed to air at r.t. the typical diffraction lines for hydrotalcite materials [53] could be detected. There are no significant differences between the two samples with Cu/Mg/Al ratios of 1:1:2 and 1:2:1, apart from a slight shift in the position of the maxima, as expected due to the change in the relative ratio of the M(II) and M(III) ions. No diffraction lines could be detected for single oxides, such as CuO, MgO or Al_2O_3. Instead weak lines of CuO could be detected in binary (Cu/Al) samples with Cu:Al = 1:2 [29].

Scanning electron microscopy images show a homogeneous distribution of all elements (Cu, Mg, Al) after calcination and EDAX analysis do not show phase segregation. Micrographs, especially after calcination and subsequent exposure to air, show the presence of large particles which are aggregates of smaller, random-oriented plate-like particles with dimensions around 50–200 nm. The samples after calcination at 500 °C and cooling in an inert atmosphere do not show apparently these platelets and are XRD-amorphous. We may thus conclude that upon exposure to air there is the formation of these platelets having probably the hydrotalcite structure, in agreement with the ''memory effect'' showed by these materials [31]. It should

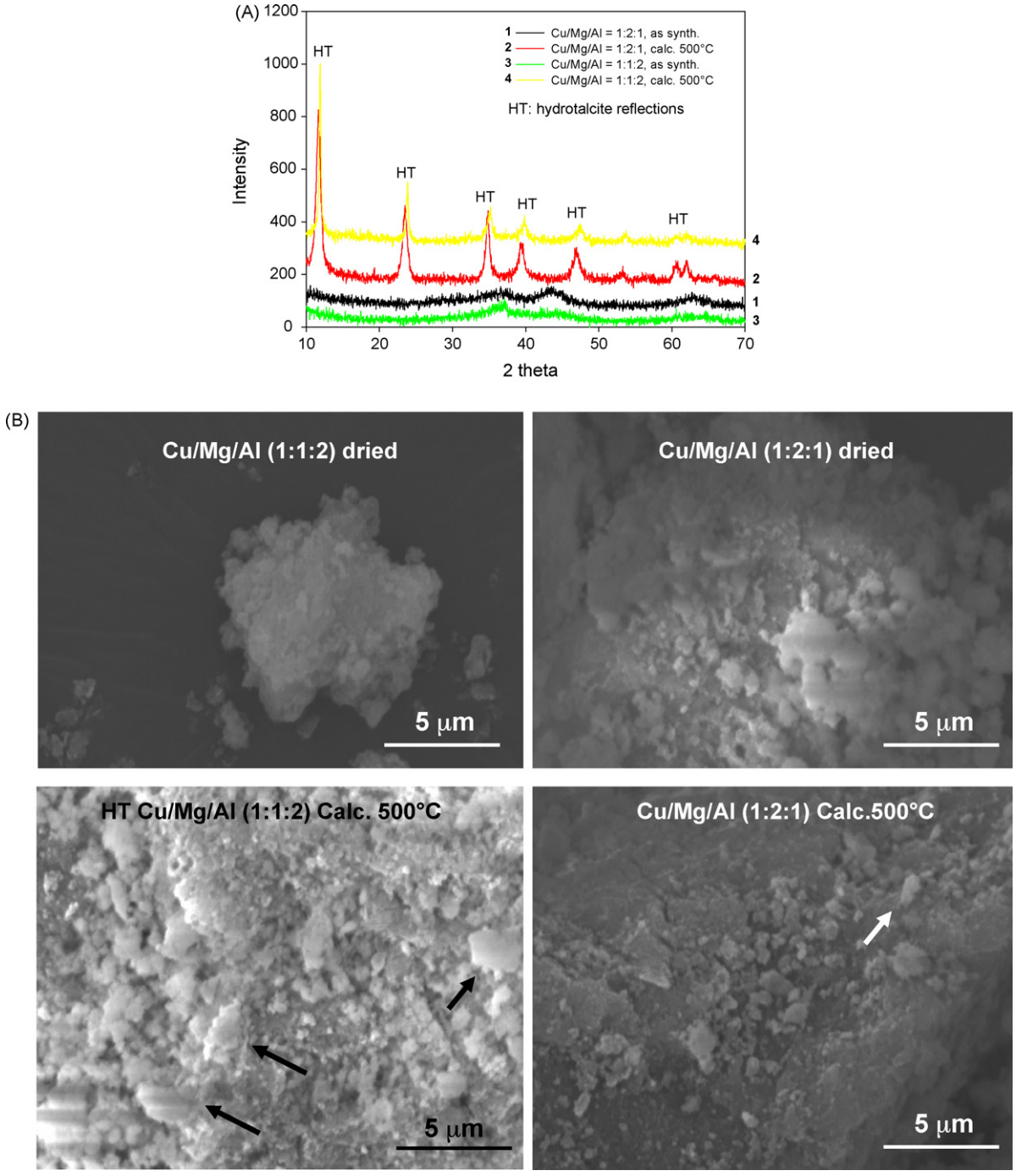

Fig. 1. (A) X-ray diffraction (XRD) pattern of ternary Cu:Mg:Al = 1:1:2 and 1:2:1 samples as synthesized (after drying), and after calcination at 500 °C and subsequent exposure to air at r.t. (B) Scanning electron microscopy (SEM) of ternary Cu:Mg:Al = 1:1:2 and 1:2:1 samples as synthesized (after drying), and after calcination at 500 °C and subsequent exposure to air at r.t.

be noted, however, at prior the reactivity tests in thermobalance or flow reactor there is a pre-treatment at 500 °C. Therefore, these hydrotalcite-like platelets probably decompose again forming an amorphous mixed oxide.

3.2. Comparison between ternary and binary HT-derived compounds

Fig. 2 reports an example of the results obtained studying the kinetic of adsorption of SO_2 at 500 °C on the two ternary and the two binary HT-samples. These tests were made in the presence of a flow of 0.1% SO_2 (1000 ppm) in air. The sorption curves are characterized by a first region where a nearly linear increase of the weight with respect to time on stream is present. A threshold value of SO_2 uptake above which the rate becomes controlled from a different kinetic control can be also evidenced. We may schematically assume that in the first linear region the kinetic regime is due the surface adsorption of SO_2, while in the second region the kinetic control is related to the solid-state diffusion of SO_x species. It should be clarified

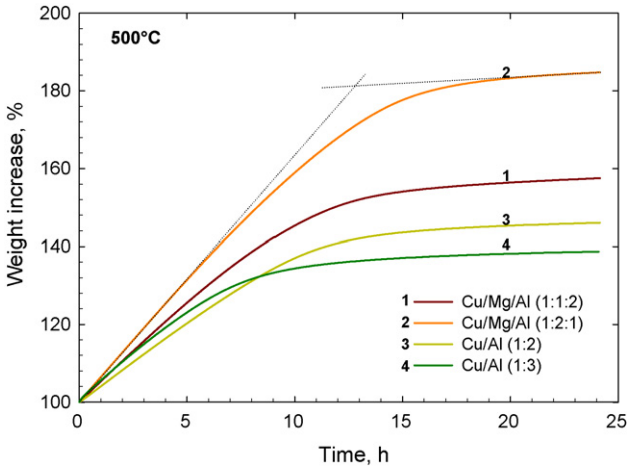

Fig. 2. SO_2 isothermal uptake curve in TG reactivity tests at 500 °C for the ternary Cu:Mg:Al = 1:2:1 and 1:1:2 and binary Cu/Al = 1:2 and 1:3 calcined samples. Feed: 0.1% SO_2 in air.

that the mechanism is more complex [29]: there is a reversible chemisorption of SO_2 and oxidation to SO_3, which may then react with surface Brönstead sites to form a surface sulphate species. The direct reaction of SO_2 with surface Brönstead sites to form a surface sulphite species, which is then oxidised to a surface sulphate species, competes with the first pathway. Different surface sulphite and sulphate species (mono- and bi-dentate, linked to Cu, Mg or Al sites or bridging two different ions, etc.) could be detected by FTIR. The surface sulphate species then progressively diffuse to bulk. Scheme 1 schematically outlines the reaction mechanism.

It should be also considered that this is a gas–solid reaction, where one of the reactants is the solid (SO_x trap). However, there are two main differences with respect to classical gas–solid reactions (carbon combustion, for example): (i) there is a first catalytic step of oxidation of SO_2 or sulphite, and (ii) the relatively high surface area and low temperature of operations (with respect to carbon combustion). Therefore, a ''shrinking-core'' model, as that used often for gas–solid reactions does not describe correctly the results [28].

Assuming a first linear region controlled by the surface adsorption of SO_2, and a second region where the kinetic control is related to the solid-state diffusion of SO_x species is thus a very rough approximation. In the context of the present discussion, however, it may be acceptable to distinguish between the two regions of different kinetic regime evidenced by thermobalance data (Fig. 2).

The change of kinetic controlling regimes occurs approximately in the 30–40% wt. increase range for the two binary

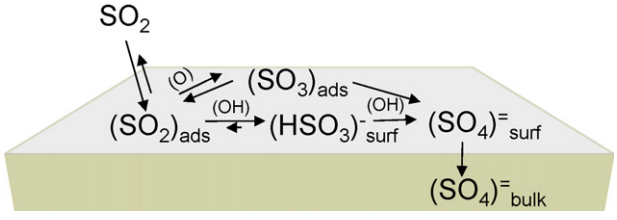

Scheme 1. Schematic mechanism of the process of SO_2 storage over SO_x traps.

reference samples having a Cu/Al ratio of 1:2 and 1:3, respectively. It reaches a value nearly 60% wt. increase for Cu/Mg/Al = 1:1:2 and nearly 80% wt. increase for Cu/Mg/Al = 1:2:1. Therefore, by introducing Mg in the Cu/Al HT-derived materials the limiting SO_2 sorption capacity is about twice of that of the binary Cu/Al HT-derived materials, evidencing the marked effect in promoting the SO_2 sorption performances. Note that this limiting SO_2 sorption capacity was about 15% wt. increase at 500 °C for a reference SO_x trap containing 2% Pt [28].

These TG data could be elaborated to derive the dependence of the rate of SO_2 uptake (μmoles SO_2 sorbed per h and per m^2 of surface area) from the total μmoles of SO_2 adsorbed per m^2 of the SO_x trap. The results for the two ternary HT-derived materials at 200, 300 and 500 °C are reported in Fig. 3a–c, respectively. The analogous results for the two reference binary samples are reported in Fig. 4a and b for Cu/Al = 1:3 and Cu/Al = 1/2, respectively. Progressively to the surface saturation by SO_x species, the process of migration of surface sulphate to the bulk of the mixed oxide particles also starts. If the bulk diffusion is faster, due to an easier structural rearrangement of the structure (the transformation from metal-oxide to metal-sulphate induces a cell volume expansion of about 30–40%), the first region of higher reaction rate extends to a higher degree of SO_2 uptake. For this reason, thermogravimetric data (Fig. 2) were normalize per m^2 of surface area, to eliminate the dependence from surface saturation.

At 200 °C the initial rate of SO_2 uptake is similar for Cu/Mg/Al = 1:2:1 and 1:1:2 (Fig. 3a), but rapidly decreases in the former and reaches a value 10 times lower for a total amount of SO_2 adsorbed of about 6–7 μmoles SO_2 m^{-2}. Instead, in Cu/Mg/Al = 1:1:2, the rate of SO_2 uptake maintains nearly constant up to a total amount of SO_2 adsorbed of about 4–5 μmoles SO_2 m^{-2} and then decreases reaching a value about then times lower than the initial one for a total SO_2 uptake of about 15–16 μmoles SO_2 m^{-2}, e.g. nearly three times that of the Cu/Mg/Al = 1:2:1 sample. Note that due to the limited difference in the surface area of the calcined ternary samples (Table 1) the results are not very different by expressing the rates per g of SO_x trap instead that per m^2, but the latter offers a more correct comparison.

With respect to binary reference Cu/Al materials (Fig. 4a and b), it may be observed that at 200 °C the behaviour of Cu/Mg/Al = 1:2:1 is only slightly better than that of Cu/Al = 1:3 sample, while significantly better with respect to Cu/Al = 1:2 sample. Cu/Mg/Al = 1:1:2 instead shows quite superior performances at 200 °C with respect to both binary samples. Worth noting is that a poor relationship could be observed between the total amount of copper per m^2 of the sample and the initial rate of SO_2 uptake (per m^2) at 200 °C (Fig. 5a). At this low temperature, the rate of SO_2 uptake should depend on the rate of oxidation of the chemisorbed SO_2 species, which in turn depends on the amount of copper sites, because this is the only element in our materials having redox properties. The poor relationship observed (Fig. 5a) indicates that the mechanism of SO_2 chemisorption is probably more complex, in agreement with previous indications [29], and/or that it may be not

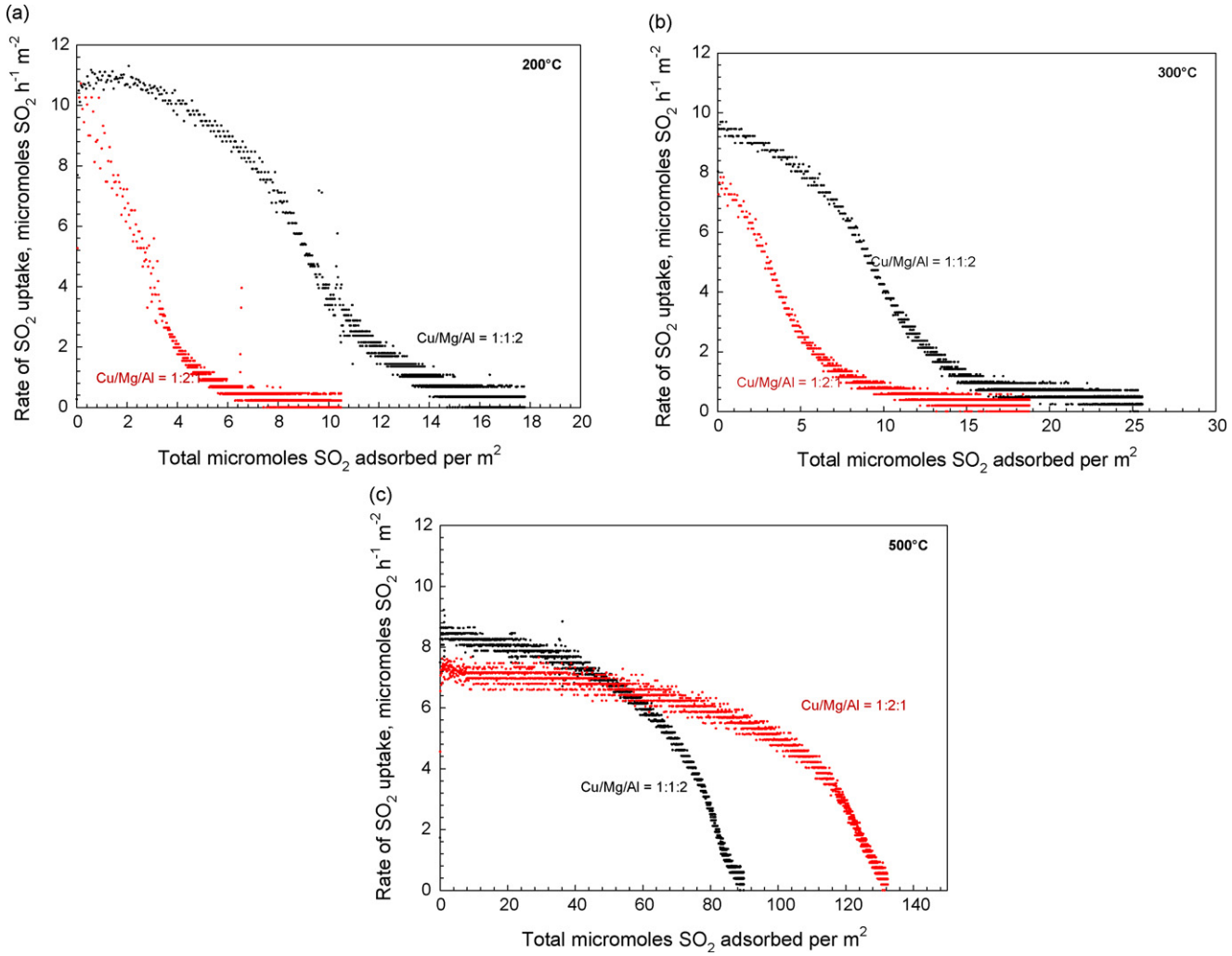

Fig. 3. Rate of SO_2 uptake per m^2 of SO_x trap (μmoles SO_2 h^{-1} m^{-2}) vs. total μmoles of SO_2 adsorbed per m^2 for the ternary Cu/Mg/Al = 1:1:2 and 1:2:1 samples: (a) 200 °C, (b) 300 °C and (c) 500 °C. Feed as in Fig. 2.

possible to make an assumption of a direct relationship between number of surface copper sites and rate of SO_2 uptake. Fig. 5a shows that a poor relationship exists between total amount of copper per m^2 of the sample and the total amount of SO_2 adsorbed at 200 °C m^{-2} of the sample.

At 300 °C (Fig. 3b) the behaviour is analogous, although the difference between the two samples is less relevant, and the initial rate of SO_2 uptake for Cu/Mg/Al = 1:1:2 is slightly higher than that of Cu/Mg/Al = 1:2:1. With respect to binary Cu/Al materials (Fig. 4a and b), where the increase of the reaction temperature between 200 and 300 °C has a minor effect, the increase of the temperature for ternary Cu/Mg/Al materials has a more pronounced positive effect, especially for the Cu/Mg/Al = 1:2:1. This indicates that magnesium participates to the reaction of SO_x uptake only at higher reaction temperatures with respect to aluminium, even if the opposite effect may be expected due to the higher basicity of magnesium with respect to aluminium.

At 500 °C (Fig. 3c) a different behaviour with respect to that observed at lower temperatures was found. The initial rate of SO_2 uptake of Cu/Mg/Al = 1:1:2 sample was slightly higher of that of Cu/Mg/Al = 1:2:1 sample and maintained nearly constant up to a total amount of adsorbed SO_2 of 40–6 μmoles m^{-2}. However, in Cu/Mg/Al = 1:2:1 sample this region of nearly constant rate of SO_2 uptake maintains up to an amount of about 80–100 total μmoles SO_2 adsorbed per m^2. As a consequence for higher values of SO_2 uptake the Cu/Mg/Al = 1:2:1 sample shows a higher rate than Cu/Mg/Al = 1:1:2. With respect to binary systems at 500 °C (Fig. 4a and b), the increase of the performances is quite relevant, with a limiting SO_2 total uptake, e.g. when the SO_2 rate of uptake becomes less than one tenth of the initial one, about 4–6 times higher.

Plotting the limiting SO_2 total uptake at 500 °C versus the total copper in the sample (both per m^2 of sample), a significant larger total SO_2 uptake is evident for ternary samples, while there is a reasonable correspondence for binary samples (Fig. 5b). The relationship is slightly better in ternary systems when plotting the limiting SO_2 total uptake at 500 °C versus the total copper + magnesium in the sample, but still there are large deviations from the linear relationship. This indicates that not only the composition determines the performances of SO_x traps, but also the effective rate of bulk diffusion of sulphate

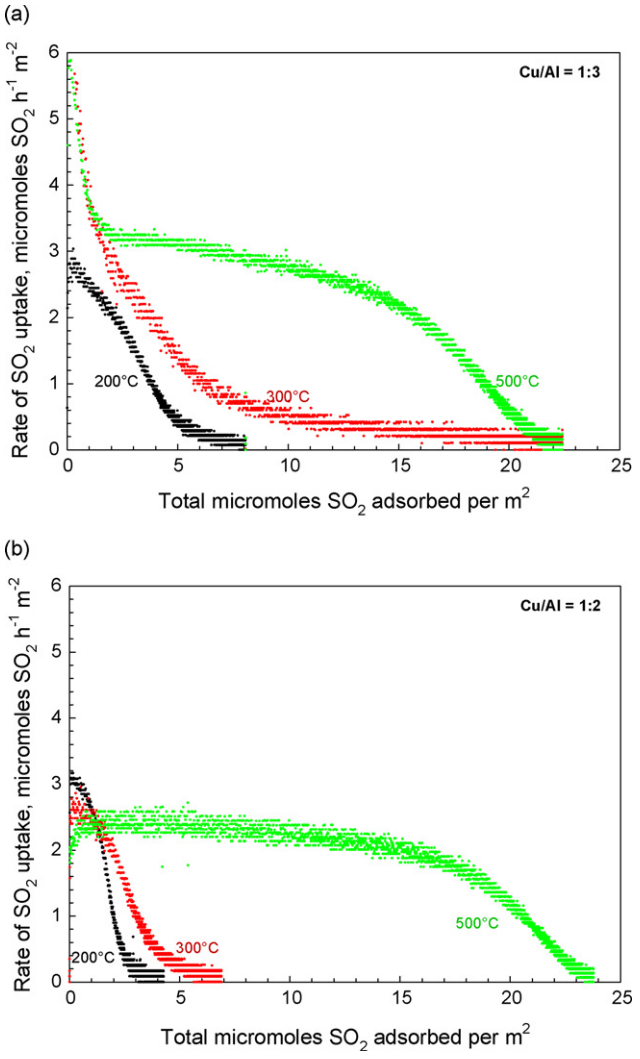

Fig. 4. Rate of SO_2 uptake per m^2 of SO_x trap (μmoles SO_2 h^{-1} m^{-2}) vs. total μmoles of SO_2 adsorbed per m^2 at different reaction temperatures for the binary Cu/Al = 1:3 (a) and Cu/Al = 1:2 (b) samples. Feed as in Fig. 2.

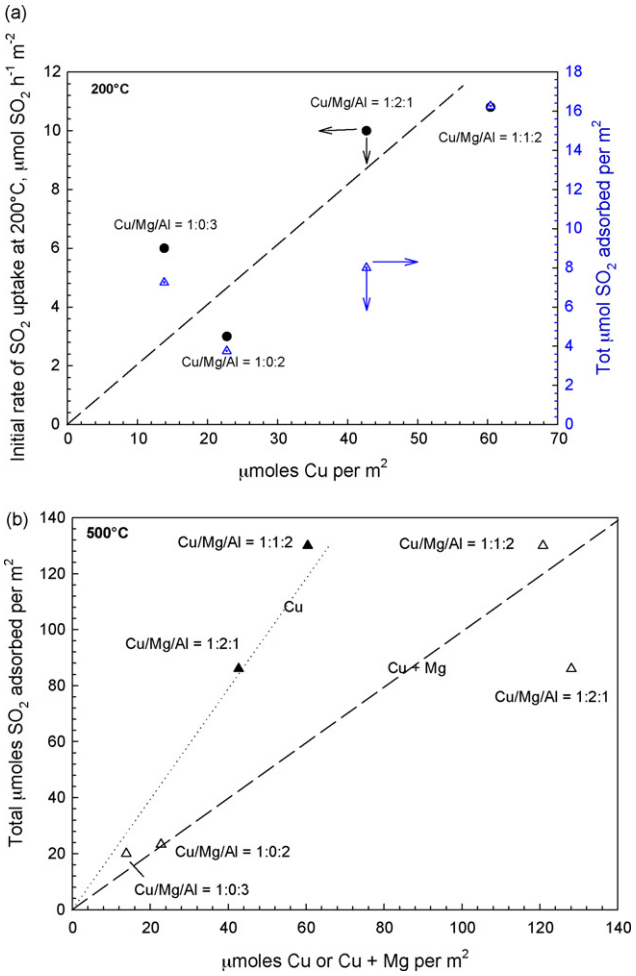

Fig. 5. (a) Initial rate (at zero time on stream) of SO_2 uptake at 200 °C m^{-2} of SO_x trap (μmoles SO_2 h^{-1} m^{-2}) vs. μmoles of copper per m^2 of SO_x trap (left/bottom axes) and total μmoles SO_2 adsorbed at 200 °C m^{-2} of SO_x trap (μmoles SO_2 m^{-2}) vs. μmoles of copper per m^2 of SO_x trap (right/bottom axes). Feed as in Fig. 2. (b) Total μmoles SO_2 adsorbed at 500 °C m^{-2} of SO_x trap (μmoles SO_2 m^{-2}) vs. μmoles copper m^{-2} of SO_x trap (full triangular symbols) or vs. μmoles of copper and magnesium per m^2 of SO_x trap (open triangular symbols). Feed as in Fig. 2.

species, which is related to the "flexibility" of the structure (which also depends on the composition) in accommodating the structural change consequent to the bulk sulphation process.

3.3. Kinetics of SO_2 uptake at low SO_2 concentration in the feed

The kinetics results in the previous section were obtained at a concentration of 1000 ppm SO_2 in air, which is relevant for applications such as in FCC, but is two orders of magnitude higher than the SO_2 concentration typically present in autoexhaust emissions (few ppm). The kinetics of sorption of SO_2 on ternary samples was thus studied using a feed of 10 ppm SO_2 in air, even if at this low concentration it is possible to study only the initial rate of adsorption, because complete saturation of SO_x sorption capacity would require extremely long reaction times (around 2000 h).

The results are summarized in Fig. 6a which reports the initial rate of SO_2 uptake as a function of the reaction temperature in the two ternary samples and the rate after adsorption of 6.25 moles - SO_2 m^{-2}. For a better comparison, the analogous graph determined for a feed of 1000 ppm SO_2 in air instead of 10 ppm SO_2 in air (Fig. 6a) is reported for the same two ternary samples (Fig. 6b). In the whole range of analyzed temperatures, the initial rate of SO_2 uptake is higher for Cu/Mg/Al = 1:1:2 samples with respect to 1:2:1 sample. However, the initial rate of SO_2 uptake increases nearly exponential with the reaction temperature at low SO_2 concentration (Fig. 6a) and decreases at higher SO_2 concentration (Fig. 6b). This could be explained considering that at high SO_2 concentration (1000 ppm) the rate of SO_2 uptake is largely dominated by a reversible chemisorption of SO_2 whose relative relevance decreases on increasing the reaction temperature, while the rate of the irreversible uptake in the form or sulphite or sulphate species increases. This is in agreement with previous observations on the reaction mechanism of SO_2 adsorption [29].

Worth to note is also that the ratio of the initial rate of SO_2 uptake using 1000 or 10 ppm of SO_2 in the feed ranges from

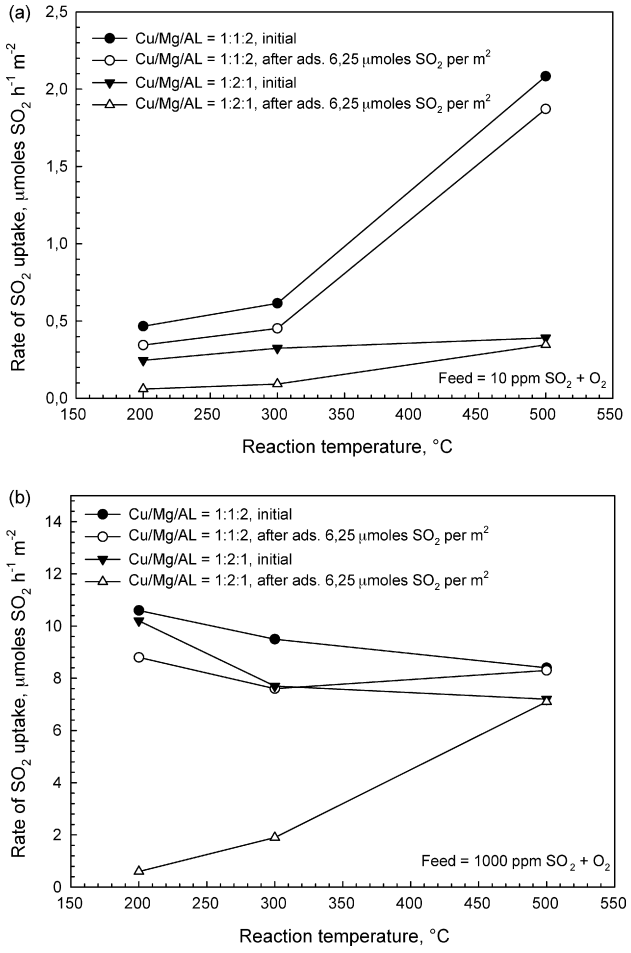

Fig. 6. Initial rate of SO_2 uptake per m^2 of SO_x trap (μmoles SO_2 h^{-1} m^{-2}) or rate after the SO_x trap has adsorbed 6.25 μmoles SO_2 per m^2 vs. reaction temperature for the ternary Cu/Mg/Al = 1:1:2 and 1:2:1 samples: (a) feed, 10 ppm SO_2 in air, (b) feed, 1000 ppm SO_2 in air.

4–5 at 500 °C to about 20 at 200 °C (for 1:1:2 sample), e.g. much less than the relative ratio of the two SO_2 concentrations. The kinetics of adsorption thus largely deviates from linearity and shows probably a saturation effect in the 50–100 ppm range.

In Cu/Mg/Al = 1:1:2 the rate of uptake of SO_2 at low SO_2 concentration (Fig. 6a) after adsorption of 6.15 μmoles SO_2 m^{-2} follows a similar trend of the initial rate with respect to the reaction temperature. This indicates that at least up to this total uptake level of SO_2 the rate is only little influenced by bulk diffusion of SO_x. This is in agreement with the kinetics observed at higher SO_2 concentration (1000 ppm, Fig. 3b).

The situation is different for the sample Cu/Mg/Al = 1:2:1, which shows a lower temperature dependence of the initial rate of SO_2 uptake, but a more pronounced sensitivity of the rate upon adsorption of 6.15 μmoles SO_2 m^{-2}. This result is in agreement with the kinetics observed at higher SO_2 concentration (1000 ppm, Fig. 3b).

Therefore, we may conclude that notwithstanding the differences in the kinetic behaviour commented above, the general trend in comparing the performances of ternary Cu/Mg/Al samples at low and higher SO_2 concentration in the feed is similar.

3.4. Breakthrough curves of SO_2 uptake

The tests in a thermobalance allow to determine precisely how the rate of SO_2 uptake changes as a function of the amount of SO_2 captured, but do not give indications neither on the performances using very short contact times of the gas with the solid nor on the effect of other components in the gas phase. For this reason, thermobalance experiments were complemented with the determination of the breakthrough curves for SO_2 capture in a flow reactor apparatus at very high space-velocity and using a feed simulating that of exhaust gas from diesel engines. Due to technical limitations connected to the use of an infrared detector and a gas cell to monitor the SO_2 present in low concentrations, these experiments were made in the absence of water vapour in the feed. However, check tests cofeeding water do not indicate a major effect of the presence of water vapour on the breakthrough curves for SO_2 capture.

Reported in Fig. 7 are the SO_2 breakthrough curves obtained at 200 °C for the two ternary Cu/Mg/Al samples showing that Cu/Mg/Al = 1:1:2 gives significantly better results than Cu/Mg/Al = 1:2:1.

Two distinct zones could be evidenced characterized by: (i) a first initial fast decrease of the efficiency in the SO_2 removal level, and (ii) a second zone for longer times on stream, which show a distinct change in the slope. This change corresponds roughly to a change in the kinetic control from ‘‘surface reaction’’ to ‘‘solid-state diffusion’’ similarly to TG experiments (Fig. 2). As commented above, this attribution for a kinetic control is used here only as indication to better discuss the results, but do not corresponds to the true kinetically controlling regime, due to the presence of various consecutive and in part reversible reactions having similar reaction rates.

These breakthrough curves could be elaborated to plot the degree of SO_2 removal as a function of the total SO_2 adsorbed per m^2. Fig. 8 reports the results for the two ternary Cu/Mg/Al samples and for the sake of comparison of the two Cu/Mg binary samples. Cu/Mg/Al = 1:1:2 shows superior performances to all samples. Cu/Mg/Al = 1:2:1 shows a behaviour

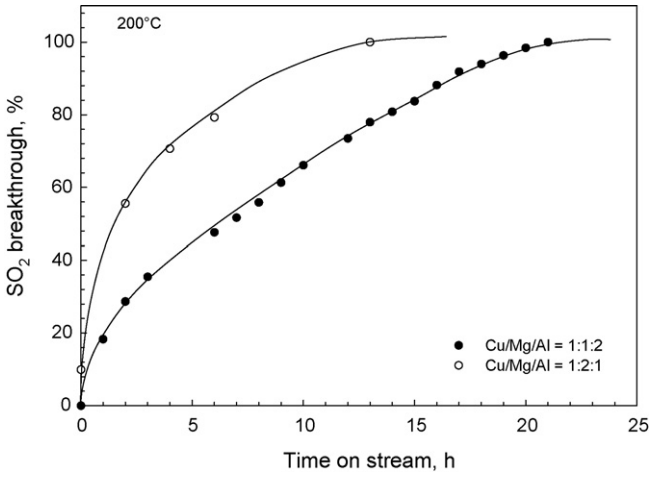

Fig. 7. Breakthrough curves of SO_2 adsorption at 200 °C for ternary Cu/Mg/Al = 1:1:2 and 1:2:1 samples. Feed: SO_2 = 0.001%, 11% CO_2, 5% O_2, and the remaining helium. Catalyst amount = 40 mg, space-velocity = 150,000 h^{-1}.

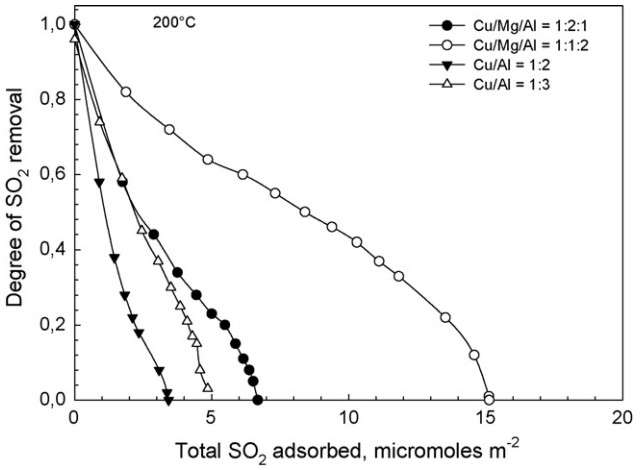

Fig. 8. Degree of SO_2 removal at 200 °C vs. total μmoles SO_2 adsorbed per m^2 of SO_x trap. Samples calcined at 500 °C.

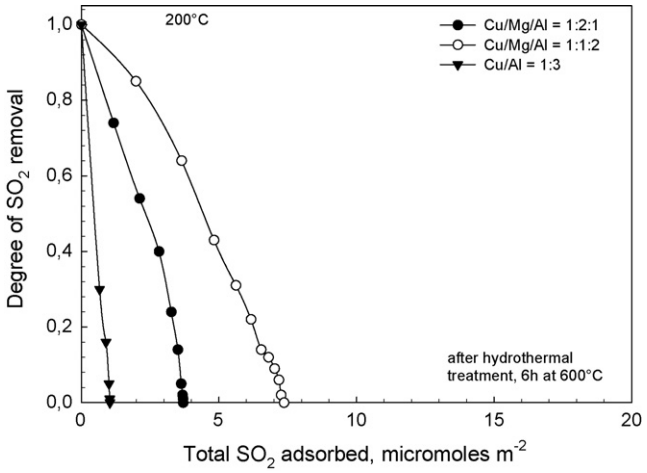

Fig. 9. Degree of SO_2 removal at 200 °C vs. total μmoles SO_2 adsorbed per m^2 of SO_x trap. Samples after hydrothermal treatment (6 h, 600 °C; see text).

comparable to that of the binary Cu/Al = 1:3 sample up to a degree of SO_2 removal equal to or higher than about 60%, e.g. when the outlet SO_2 concentration from the reactor is lower than 12 ppm. Above this threshold value, e.g. lower levels of SO_2 removal, better performances were instead observed. For all the levels of SO_2 removal the binary Cu/Al = 1:2 shows the worst performances between the studied samples.

There is thus a general agreement, but not full consistency, in the comparison of the performances of these samples obtained by measuring the SO_2 breakthrough curve in a flow reactor (Fig. 8) and the kinetics in the thermobalance apparatus (Figs. 3–5). This effect could be attributed to the presence of about 11% CO_2 in breakthrough curve experiments, which can compete with SO_2 adsorption. However, preliminary tests in the absence of CO_2 indicated that not only this factor is important, but also the use of high space-velocities (short contact times) which influence the relative rates of surface processes outlined in Scheme 1. Previous results on the reaction mechanism of SO_2 adsorption over Cu/alumina samples were in agreement with these indications [54].

The results were not markedly different from those at 200 °C at higher reaction temperatures, apart from a higher total amount of SO_2 adsorbed. They will be thus not reported here for conciseness.

3.5. Resistance to hydrothermal treatment

The analysis of the performances after hydrothermal treatment is important to understand the stability of the SO_x traps during real operations, either when applied to autoexhaust emissions or as additives in FCC. Fig. 9 reports the degree of SO_2 removal as a function of the total SO_2 adsorbed per m^2 in the same conditions of those reported in Fig. 8, but after a severe hydrothermal treatment (6 h at 600 °C, see experimental conditions) of the ternary or binary samples.

The comparison of the results reported in Fig. 9 with those in Fig. 8 shows that a general significant lowering of the SO_x trap performances after the hydrothermal treatment, especially for the binary Cu/Al = 1:3 system which lose about 80% of the total SO_2 sorption capacity which reduces to about 1/5 of the original value. In the ternary Cu/Mg/Al systems the decrease of total sorption capacity is lower (total SO_2 sorption capacity halves, e.g. reduces of about 50%), indicating that the presence of Mg increases not only the performances, but also the resistance to hydrothermal deactivation.

It may be also noted that the behaviour up to about 40% of degree of SO_2 removal, e.g. for reactor outlet concentrations less than 8 ppm SO_2, is not significantly affected by the hydrothermal behaviour which instead depresses the performances for higher levels of total adsorbed SO_2, e.g. when the bulk diffusion of sulphate is dominating the kinetics. This result suggests that the hydrothermal treatment influences mainly the rate of formation of bulk sulphate species rather than surface process.

4. Conclusions

Cu/Mg/Al ternary HT-derived materials show enhanced SO_x trap performances with respect to binary Cu/Al HT-derived materials, which already were shown to possess good SO_x trap performances in comparison to a commercial SO_x trap based on 2% Pt supported on alumina and doped with various alkaline and alkaline-earth metals [29]. Worth noting is that these HT-derived materials do not contain noble metals and may be prepared using cheap components. Therefore, Cu/Mg/Al ternary materials represent an interesting type of SO_x traps either to protect NO_x traps from the deactivation by sulphur or as SO_x additives in FCC applications.

The kinetics of SO_2 uptake was studied both at low (10 ppm) and higher (1000 ppm) SO_2 concentration in a thermobalance (TG) apparatus, and compared with the results obtained by measuring the SO_2 breakthrough curves in a flow reactor apparatus under reaction conditions simulating those of autoexhaust gases, in particular regarding the use of high space-velocities and presence of CO_2 in the feed.

The feed composition and type of experiments and/or experimental apparatus influence the SO_x trap performances, but in general it was noted that the order of reactivity and the

ranking of the SO_x trap performances were similar in the different configurations. Better performances were obtained using the Cu/Mg/Al = 1:1:2 sample which was demonstrated to have also improved hydrothermal stability with respect to Cu/Al binary samples.

Also the Cu/Mg/Al = 1:2:1 sample showed improved performances and hydrothermal stability with respect to Cu/Al binary samples, although its SO_x trap performances were lower than those of the Cu/Mg/Al = 1:1:2 sample. Therefore, the introduction of Mg in the Cu/Al HT-derived samples enhances performances and hydrothermal stability. The analysis of the dependence of the rate of SO_2 uptake from the amount of SO_2 adsorbed indicates that not only the composition determines the performances of SO_x traps. The effective rate of bulk diffusion of sulphate species, which is related to the ''flexibility'' of the structure (which also depends on the composition) in accommodating the structural change consequent to the bulk sulphation process, is another important parameter. The results presented here provide some evidences on these aspects, which, however, should be studied in more detail.

Finally, it may be concluded indicating that the experiments reported here provide some indications on how the Mg/Al ratio in ternary Cu/Mg/Al HT-derived systems affects the kinetic controlling regime and the dependence on the reaction temperature and the total amount of captured SO_2. This is an important element to improve the performances of these SO_x traps for applications either in protecting NO_x traps in autoexhaust uses or for FCC applications.

Acknowledgements

The financial support of EU (contract G3RD-CT2002-00793 NANOSTRAP) is gratefully acknowledged. The work was also realized in the frame of the activities of the Network of Excellence IDECAT NMP3-CT-2005-011730 (Integrated Design of Nanostructured Catalytic Materials for a Sustainable Production).

References

[1] R. McCabe, W. Chun, G. Graham, C. Montreuil, B. Carberry, A. Chigapov, A. Dubkov, USA, U.S. Pat. Appl. Publ., US 2,005,145,827 (2005).
[2] K. Yoshida, Toyota Jidosha Kabushiki Kaisha, Japan, PCT Int. Appl., WO 2,006,109,889 (2006).
[3] K. Kato, Toyota Motor Corp., Japan, Jpn. Kokai Tokkyo Koho, JP 2,006,138,213 (2006).
[4] K. Yoshida, S. Hirota, Y. Nakano, Toyota Jidosha Kabushiki Kaisha, Japan, PCT Int. Appl., WO 2,005,040,571 (2005).
[5] A.N. Chigapov, A.A. Dubkov, B.P. Carberry, C.N. Montreuil, G.W. Graham, R.W. McCabe, W. Chun, Ford Global Technologies, Inc., USA, Eur. Pat. Appl., EP 1,374,978 (2004).
[6] K. Nakatani, S. Hirota, Y. Henda, K. Itoh, T. Asanuma, K. Kimura, S. Toshioka, Y. Nakano, A. Mikami, Toyota Jidosha Kabushiki Kaisha, Japan, U.S. Pat. Appl. Publ., US 2,003,196,429 (2003).
[7] Z. Hu, P.L. Burk, S.-L.F. Chen, Engelhard Corporation, USA, U.S. Pat. Appl. Publ., US 2,003,175,192 (2003).
[8] M. Deeba, J.K. Hochmuth, U. Dahle, S. Brandt, Engelhard Corporation, USA, U.S. Pat. Appl. Publ., US 2,003,039,597 (2003).
[9] S. Calvo, Renault, Fr., Fr. Demande, FR 2,819,549 (2002).
[10] Z. Hu, P.L. Burk, S.-L.F. Chen, USA, U.S. Pat. Appl. Publ., US 2,002,103,078 (2002).
[11] W. Boegner, J. Guenther, H.-P. Holzt, B. Krutzsch, S. Renfftlen, C. Schoen, D. Voigtlaender, M. Weibel, G. Wenninger, Daimlerchrysler A.-G., Germany, Ger. Offen., DE 19,960,430 (2001).
[12] H.L. Fang, J.C. Wang, R.C. Yu, C.Z. Wan, K. Howden, Society of Automotive Engineers (SAE Papers), SP-1801 (Emissions: Advanced Catalyst and Substrates, Measurement and Testing, and Diesel Gaseous Emissions) (2003) 185.
[13] E. Schreier, R. Eckelt, M. Richter, R. Fricke, Appl. Catal. B: Environ. 65 (2006) 249.
[14] H. Dathe, A. Jentys, P. Haider, E. Schreier, R. Fricke, J.A. Lercher, Phys. Chem. Chem. Phys. 8 (2006) 1601.
[15] K. Tikhomirov, O. Kroecher, M. Elsener, M. Widmer, A. Wokaun, Appl. Catal. B: Environ. 67 (2006) 160.
[16] H. Dathe, E. Peringer, V. Roberts, A. Jentys, J.A. Lercher, Comptes Rendus Chimie 8 (2005) 753.
[17] H. Dathe, C. Sedlmair, A. Jentys, J.A. Lercher, Stud. Surf. Sci. Catal. 154C (2004) 3003 (Recent Advances in the Science and Technology of Zeolites and Related Materials).
[18] H. Dathe, A. Jentys, J.A. Lercher, Phys. Chem. Chem. Phys. 7 (2005) 1283.
[19] H. Dathe, A. Jentys, J.A. Lercher, J. Phys. Chem. B 109 (2005) 21842.
[20] H. Dathe, P. Haider, A. Jentys, J.A. Lercher, J. Phys. Chem. B 110 (2006) 10729.
[21] H. Dathe, P. Haider, A. Jentys, J.A. Lercher, J. Phys. Chem. B 110 (2006) 26024.
[22] L. Li, D.L. King, Ind. Eng. Chem. Res. 44 (2005) 168.
[23] L. Limousy, H. Mahzoul, J.F. Brilhac, P. Gilot, F. Garin, G. Maire, Appl. Catal. B: Environ. 42 (2003) 237.
[24] J. Wang, Z. Zhu, C. Li, J. Mol. Catal. A: Chem. 139 (1999) 31.
[25] S. Iretskaya, M.B. Mitchell, J. Phys. Chem. B 107 (2003) 4955.
[26] Y.G.G. Hao, B.R. Cooper, Surf. Sci. 312 (1994) 250.
[27] (a) G. Centi, N. Passarini, S. Perathoner, A. Riva, Ind. Eng. Chem. Res. 31 (1992) 1947;
(b) G. Centi, N. Passarini, S. Perathoner, A. Riva, Ind. Eng. Chem. Res. 31 (1992) 1956.
[28] G. Centi, S. Perathoner, Catal. Today 112 (2006) 174.
[29] G. Centi, S. Perathoner, Appl. Catal. B: Environ. 70 (2007) 172.
[30] (a) J.T. Kloprogge, D. Wharton, L. Hickey, R.L. Frost, Am. Mineral. 87 (2002) 623;
(b) Q.-Z. Jiao, Y. Zhao, H. Xie, D.G. Evans, X. Duan, Yingyong Huaxue 19 (2002) 1011.
[31] (a) F. Basile, A. Vaccari, in: V. Rives (Ed.), Layered Double Hydroxides, Nova Science Publishers, Inc., Huntington, NY, 2001, p. 285;
(b) F. Cavani, F. Trifiro, A. Vaccari, Catal. Today 11 (1991) 173.
[32] (a) D.L. Guttridge, J. Li, R.G. Hurley, R.J. Kudla, W.L.H. Watkins, Ford Global Techn. Inc., US, US Patent 2,003,129,124 (2003).;
(b) D.L. Guttridge, J. Li, M.S. Chattha, R.J. Kudla, W.L.H. Watkins, Ford Global Techn. Inc., US, EP Patent 1,304,156 (2003).
[33] (a) G. Centi, G. Fornasari, G. Gobbi, M. Livi, F. Trifirò, A. Vaccari, Catal. Today 73 (2002) 287;
(b) G. Fornasari, M. Livi, F. Trifirò, A. Vaccari, L. Balduzzi, F. Prinetto, G. Ghiotti, G. Centi, Catal. Today 75 (2002) 421–429.
[34] F. Basile, G. Fornasari, M. Livi, F. Tinti, F. Trifiro, A. Vaccari, Top. Catal. 30/31 (2004) 223.
[35] J. Yang, W. Cheng, X. Yu, L. Liu, X. Liang, C. Liu, W. Wang, X. Duan, East China Normal University, Peoples Republic of China, China Patent, Faming Zhuanli Shenqing Gongkai Shuomingshu, CN 1,883,794 and CN 1,727,052 (2006).
[36] R. Cuevas, M.T. Bueno, J. Ramirez, C. Salcedo, B. Mar, F. Pedraza, Revista Mexicana de Ingenieria Quimica 2 (2003) 1.
[37] A. Corma, A.E. Palomares, F. Rey, F. Marquez, J. Catal. 170 (1997) 140.
[38] A.E. Palomares, J.M. Lopez-Nieto, F.J. Lazaro, A. Lopez, A. Corma, Appl. Catal. B: Environ. 20 (1999) 257.
[39] B. Wen, M. He, C. Costello, Energy Fuels 16 (2002) 1048.
[40] G.L. Zhuo, Y.F. Chen, Z.H. Ge, X.Z. Jiang, Chin. Chem. Lett. 13 (2002) 279.

[41] Y. Chen, Z. Ge, D. Lu, Huanjing Kexue Xuebao 21 (2001) 307.
[42] T.J. Pinnavaia, J. Amarasekera, Michigan State University, USA, U.S. Patent, US 5,358,701 (1994).
[43] M.-X. Yu, J.-C. Xu, X.-H. Li, L.-F. Wang, Gongye Cuihua 12 (2004) 1.
[44] L. Jia, Y. Qin, Z. Ma, Z. Liang, Huaxue Tongbao 66 (2003) 435.
[45] R.E. Roncolatto, M.J.B. Cardoso, Y.L. Lam, M. Schmal, Ind. Eng. Chem. Res. 45 (2006) 2646.
[46] V.D. Dimitriadis, I.A. Vasalos, Ind. Eng. Chem. Res. 31 (1992) 2741.
[47] I.A. Vasalos, E.G. Wollaston, Standard Oil Co., USA, U.S. Patent, US 4,440,632 (1984).
[48] I.A. Vasalos, E.R. Strong, C.K.R. Hsieh, G.J. D'Souza, in: Proceedings—Refining Department, vol. 56, American Petroleum Institute, 1977 , p. 182.
[49] I.A. Vasalos, E.R. Strong, C.K.R. Hsieh, G.J. D'Souza, Oil Gas J. 75 (1977) 141.
[50] J.-O. Barth, A. Jentys, E.F. Iliopoulou, I.A. Vasalos, J.A. Lercher, J. Catal. 227 (2004) 117.
[51] E.F. Iliopoulou, E.A. Efthimiadis, I.A. Vasalos, J.-O. Barth, J.A. Lercher, Appl. Catal. B: Environ. 47 (2004) 165.
[52] E.F. Iliopoulou, E.A. Efthimiadis, L. Nalbandian, I.A. Vasalos, J.-O. Barth, J.A. Lercher, Appl. Catal. B: Environ. 60 (2005) 277.
[53] R. Allmann, H.P. Jepsen, Neues Jahrbuch fur Mineralogie, Monatshefte (1969) 544.
[54] (a) M. Waqif, O. Saur, J.C. Lavalley, S. Perathoner, C. Centi, J. Phys. Chem. 95 (1991) 4051;
(b) J.C. Lavalley, A. Janin, J. Preud'homme, React. Kinet. Catal. Lett. 18 (1982) 85.